

Gravitational Waves from Hyper-Accretion onto Nascent Black Holes

Rafael Angel Araya-Góchez

Theoretical Astrophysics MC 130-33, California Institute of Technology, Pasadena CA 91125 arayag@tapir.caltech.edu

ABSTRACT

We examine the possibility that hyper-accretion onto newly born, black holes occurs in highly intermittent, non-asymmetric fashion favorable to gravitational wave emission in a neutrino cooled disk. This picture of near-hole accretion is motivated by magneto-rotationally induced, ultra-relativistic disk dynamics in the region of the flow bounded from below by the marginally bound geodesic radius r_{mb} . For high spin values, a largely coherent magnetic field in this region has the dynamical implication of compact mass segregation at the displacement nodes of the non-axisymmetric, MRI modes. When neutrino stress competes favorably for the disk dynamical structure, the matter clumps may be rather dense and sufficiently long-lived to excite the Quasi-Normal Ringing (a.k.a. QNR) modes of the Kerr geometry upon their in-fall. We find that such accretion flow may drive bar-like, quadrupole ($l, m = 2, 2$) modes in nearly resonant fashion for spin parameters $a \geq .9$. The ensuing build up in strain amplitude of the undamped oscillations warrants a brisk rate of energy deposition into gravitational waves. A detectability assessment for the LIGO interferometers through the match filtering technique is given by integrating the energy flux over a one second epoch of resonant hyper-accretion at $1 M_{\odot} \text{ sec}^{-1}$. Thus, a $15 M_{\odot}$ Kerr black hole spinning at $a \simeq .98$ ($f_{\text{QNR}} \simeq 1677 \text{ Hz}$), and located at 27 Mpc (e.g., GRB980425), will deliver a characteristic strain amplitude, $h_{\text{char}} \simeq 2.2_{-21}$, large enough to be detectable by LIGO II. If resonant hyper-accretion were sustainable for a longer period (or at higher rates) possibly associated with a second broad hump in a GRB light-curve, these objects could be detected by LIGO I at very low redshifts.

Key words: MHD—instabilities—black hole physics—gravitational waves

1 INTRODUCTION

It seems only fitting for ultra-relativistic, black hole accretion to be the leading contender to energize and explode the massive stars associated with gamma-ray bursts and hyper-novæ. One must recognize, however, that such a scenario resides on a very exotic front: stellar-mass black holes accreting at twelve orders of magnitude above the Eddington limit! On the other hand, since GRB engines are effectively hidden from view, gravitational wave emission models may constitute the most effective probes to such enigmatic events. Indeed, there is a great deal of impetus to address such extreme accretion scenario and its associated, non-standard energy deposition channels. In this paper we are chiefly concerned with the possibility that the dynamical structure of hyper-accreting flows is highly intermittent on large scales, with the in-fall of large mass over-densities leading to prolific gravitational wave emission coincident with the gamma-ray stage.

We envisioned the accretion disk setting following the hyper-accreting black hole models of Popham, Woosley & Fryer (1999, hereafter PWF). For a fiducial scenario: $M_h = 3 M_{\odot}$, $\alpha_{\text{SS}} = 0.1$, and $\dot{M} = 0.1 M_{\odot} \text{ sec}^{-1}$, these authors found that the onset of photo-disintegration and of neutrino cooling at radii $r \lesssim 70 [GM/c^2]$ yield a mildly advective, semi-thin, $\mathcal{H}_{\Theta}/r \lesssim .4$, accretion disk structure with a slightly sub-Keplerian rotation profile. An improved account of neutrino transport (Di Matteo *et al.* 2002) has found that the innermost disk portion should become optically thick to neutrinos for accretion rates $\dot{M} \gtrsim 0.1 M_{\odot} \text{ sec}^{-1}$. This being the case, cooling by radial advection of energy will compete with that from local neutrino emission and advection will overwhelm neutrino cooling for $\dot{M} \gtrsim 1 M_{\odot} \text{ sec}^{-1}$ (Di Matteo *et al.* 2002). Yet, such a high accretion rate is rather unlikely (MacFadyen *et al.* 2001), so we restrict our analysis to $\dot{M} \leq 1 M_{\odot} \text{ sec}^{-1}$.

The structure of this paper is as follows. In §2, we assess the relevance of physical processes occurring in the relativistic region of the flow: $r_{\text{mb}} \leq r \leq r_{\text{ms}}$. Magneto-rotationally-induced, relativistic disk dynamics is addressed in §3, where we also discuss the role of compressibility and estimate the size of mass over-densities from a neutrino cooled disk. In §4 we build an idealized, analytical model for gravitational wave emission and, in §5, estimate the detectability of the GW signal for the LIGO interferometers with the match filtering technique.

2 PHYSICS INSIDE THE ISCO

The model for gravitational wave emission outlined in §4 is based on the premise that large-scale magneto-rotational effects will drive the disk dynamics in the ultra-relativistic region of the flow bounded from below by the marginally bound orbit radius. For spin rates $a \geq .9$, the growth rate of the magneto-rotational instability σ_{MRI} (a.k.a. MRI), is faster than the inverse dynamical time scale, Ω_+^{-1} , throughout the annulus $r_{\text{mb}} \leq r \leq r_{\text{ms}}$ by a factor $\simeq \mathcal{O}[2]$ (see Fig 1). Thus, a small delay to reach the “free-fall” stage is all that is needed for magneto-rotational dynamics to take place. On the other hand, r_{mb} represents the lowest bound on the location of the cusp in effective potential and is akin to a relativistic generalization of the inner Lagrangian point, L_1 , for mass transfer in close binaries (Kozłowski, Jaroszyński & Abramowicz 1978).

The exact location of the inner boundary depends on the source of free-energy for the flow. Standard lore holds that the flow draws energy from the radial gradient in angular momentum and that since dissipation of angular momentum vanishes at r_{ms} for a Keplerian disk, this is where the inner edge of such a disk should reside (Novikov & Thorne 1973). Yet, we now know that when the disk dynamics is driven by magneto-rotational effects the source of free energy is not the gradient in the radial distribution of angular momentum but rather the gradient in angular velocity¹; that is, the source of free-energy is the shear of the congruence of circular geodesics. Thus, MRI-mediated, turbulent angular momentum transport goes on unabated at the radius of marginal stability for cold geodesic orbits (Araya-Góchez 2002) and the flow within need not preserve specific angular momentum *nor* lose its relativistic Keplerian rotation profile in spite of a non-trivial radial velocity.

We will therefore assume a Keplerian angular velocity profile throughout: $r \geq r_{\text{mb}}$. This assumption is consistent with the models of PWF and Popham & Gammie (1999)—indeed, strong deviations from Keplerian rotation only occur as fluid elements approach the photon radius r_{ph} —and it is also consistent with global 3D simulations of non-radiative MHD accretion onto non-spinning black holes (Hawley & Krolik 2001, Hawley & Balbus 2002) in spite of partial pressure support for hot inner tori.

Inside r_{ms} , the flow may not have time to cool significantly and advection of entropy will become progressively more important as the horizon, r_+ , is approached. Entirely advective, accretion flows (i.e., non-radiative, hydrodynamical flows) are reckoned to possess a large, positive Bernoulli function $\mathcal{B} = \varrho + \int_0^p dp \rho/\varrho$ (Abramowicz *et al.* 1978, Blandford & Begelman 2003) which makes the ultimate fate of accreting fluid particles a theme of controversy; e.g., ADAF (Narayan & Yi 1995) *vs* CDAF (Narayan *et al.* 2000) *vs* ADIOS (Blandford & Begelman 1999, 2003). The broad conclusion drawn from this ongoing debate is that fluids with large internal energies, e.g., strongly magnetized fluids, are not easily accreted onto gravitational wells. In the ultra-relativistic flows of interest to us, and for large spin parameter a , the value of the relativistic enthalpy, $\varrho \equiv (\rho + \varepsilon + p)$, can be non-trivial $\varrho/\rho \geq 2$ (with magnetic energy folded into the internal energy ε), implying a high likelihood for large Bernoulli function as well. We adopt the view that for a fluid with such high enthalpy, the dynamical boundaries set by the circular orbits of *cold* (point) particles in the Kerr geometry are inadequate.

3 MAGNETO-ROTATIONALLY-INDUCED RELATIVISTIC DISK DYNAMICS

The MRI enables accretion through vigorous, turbulent transport of angular momentum. It also constitutes the key process to tap the free-energy available in a flow endowed with differential rotation. In the Newtonian picture, this is essentially a local, co-moving instability as the interplay of inertial accelerations with the elastic coupling of fluid elements creates an unstable situation to the redistribution of specific angular momentum, $\ell(r)$, if the *angular velocity profile* decreases monotonically with radius. This criterion is in opposition to the (non-magnetic) Rayleigh criterion for stability of a differentially rotating fluid: $r^{-3} d_r \ell^2 = \kappa^2 \geq 0$, where κ is the frequency of radial epicyclic motions. Indeed, without the elastic coupling provided by the bending of field lines, such inertial forces—namely, the shear(tide) and the coriolis terms—induce radial epicyclic motions while preserving specific angular momentum.

Incompressible MRI initiated turbulence has a characteristic “parallel” scale for fastest growing modes corresponding to $k_{\parallel} \equiv \mathbf{k} \cdot \mathbf{1}_{\mathbf{B}} \simeq \Omega/v_{\text{Aif}}$, and a normalized growth rate $\sigma = \hat{\mathbf{A}} \equiv \frac{1}{2} d_{\ln r} \ln \Omega$, associated with the shear parameter, a.k.a. the Oort A “constant”. Although slower growing modes occur at larger scales, we take the fastest growing modes to be the dynamically predominant eddies given that the radial flow velocity is non-negligible in $r_{\text{mb}} \leq r \leq r_{\text{ms}}$. Thus, the scale associated with the MRI is generally smaller than the vertical scale height of the disk by a factor $\mathcal{O}[v_{\text{Aif}}/c_{\mathcal{H}}]$ and no large-scale effects are expected. Indeed, in the weak field limit one may construct a dispersion relation quite independently of the large-scale field topology: highly sub-thermal fields, $v_{\text{Aif}}/c_{\mathcal{H}} \ll 1$, guarantee that the instability is truly local and incompressible (see below). When the field is more moderate, k_{\parallel}^{-1} will approach the disk’s pressure scale height $\mathcal{H} \simeq c_{\mathcal{H}}/\Omega$, and this imposes a lower bound on k_{\parallel} when the field is mostly vertical. On the other hand, the lowest bound on k_{\parallel} in a toroidal field geometry is $1/r$ which would correspond to a supra-thermal field in the Newtonian picture (Foglizzo & Tagger 1995, hereafter FT). Because of the possibility of large-scale, global disk dynamics, these modes are the focus of our analysis below.

¹ More generally, Balbus (2002) has found that for a magneto-rotationally-driven disk, the proper replacement of the classical Høiland stability criteria for rotational and convective motions involves the gradients in angular velocity and temperature instead of angular momentum and entropy.

3.1 Compressible Non-axisymmetric MRI modes

In the 2D regime of fastest growth, $k_\theta \gg k_r \gg k_\varphi$, non-axisymmetric “horizontal” displacement modes of a toroidal field have the following dispersion relation (Araya-Góchez 2002)

$$\hat{\sigma}^4 - \{(\Lambda + 1)\hat{q}_B^2 + \hat{\chi}^2\} \hat{\sigma}^2 + \Lambda \hat{q}_B^2 \{\hat{q}_B^2 + 4\hat{\Lambda}\} = 0, \quad (1)$$

where all frequencies are normalized to the rotation rate, $\hat{\Lambda} \equiv \frac{1}{2}d_{\ln r} \ln \Omega$ is the Oort A “constant”, $\hat{\chi}^2 \equiv 4(1 + \hat{\Lambda})$ is the squared of the epicyclic frequency, and $\hat{q}_B \equiv (\mathbf{k} \cdot \mathbf{v}_{\text{Alf}})/\Omega$ is a frequency related to the component of the wave vector along the field (in velocity units).

Λ is defined through

$$\Lambda \equiv \frac{\Gamma}{\Gamma + \Theta} \quad (2)$$

where Γ is the adiabatic index, and $\Theta \equiv v_{\text{Alf}}^2/c_{\mathcal{H}}^2$. This definition entrains an important anisotropy constraint on the Lagrangian displacement vector field $\boldsymbol{\xi} : v_{\text{Alf}}^2 (\mathbf{k}_\perp \cdot \boldsymbol{\xi}_\perp) = -c_s^2 (\mathbf{k} \cdot \boldsymbol{\xi})$, as well as the compressibility characteristics of non-axisymmetric modes (as a function of the component of Lagrangian displacement along the field, Foglizzo and Tagger 1995):

$$\frac{\Delta\rho}{\rho} = (1 - \Lambda) (-ik_\parallel \xi_\parallel) \quad (3)$$

where Δ denotes the Lagrangian (co-moving) perturbation as opposed to the Eulerian perturbation δ (recall the non-relativistic relation $\tilde{\Delta} = \delta + \boldsymbol{\xi} \cdot \nabla$). Evidently, the compressibility of the modes is imprint on the deviations of Λ from unity. A word of caution here regards the peculiar behavior of the fluid when the internal stress has heat conduction characteristics, e.g. photon or neutrino pressure; see §3.3. From Eq [3], one reads that the degree of compression of the modes gets stronger with the field strength and, naturally, with a softer equation of state. Note that setting $\Lambda \doteq 1$ in the dispersion relation Eq [1] yields the incompressible, local variant of the MRI.

From the dispersion relation Eq [1], one finds the parallel wave-numbers of fastest growth to satisfy (see also Foglizzo 1995)

$$\hat{q}_B^2 = -2\hat{\Lambda} + \left(\frac{1+\Lambda}{2\Lambda}\right) \times \left\{-\frac{2\Lambda\hat{\Lambda}^2}{D}\right\} \xrightarrow{\Lambda \rightarrow 1} -\hat{\Lambda}(2 + \hat{\Lambda}), \quad \text{where } D \equiv 1 + \left(\frac{1-\Lambda}{2}\right)\hat{\Lambda} + \sqrt{1 + (1 - \Lambda)\hat{\Lambda}}, \quad (4)$$

while the expression in the curly brackets corresponds to the square of the growth rate.

3.2 General Relativistic Effects in the Cowling Limit

General relativity modifies this Newtonian results in that it introduces large-scale effects when shear begins to overwhelm the coriolis terms, i.e., as r_{ph} is approached (see Eqs [32] of Araya-Góchez 2002). Although the hole is likely to be born in an excited state, e.g., away from its asymptotic, Kerr geometry; we work in the Cowling limit, $\delta g \doteq \emptyset$, and, to zeroth order, use the standard form of the Kerr metric in the equatorial plane (Boyer-Lindquist coordinates):

$$ds^2 = -\frac{D}{A} dt^2 + r^2 \mathcal{A} (d\varphi - \omega dt)^2 + \frac{1}{D} dr^2, \quad (5)$$

with $\omega \equiv 2a/\mathcal{A}r^3$ the rate of frame dragging by the hole and where the metric functions of the radial **BLF** coordinate are written as relativistic corrections (e.g. Novikov and Thorne 1973):

$$\mathcal{A} \equiv 1 + \frac{a^2}{r^2} + 2\frac{a^2}{r^3}, \quad \text{and } \mathcal{D} \equiv 1 - \frac{2}{r} + \frac{a^2}{r^2},$$

in normalized geometrical units ($c = G = M_{\text{bh}} = 1$).

For circular, incompressible, geodesic flow, the dispersion relation near a rotating hole is given by (Araya-Góchez 2002)

$$(\gamma\sigma)^4 - [2\hat{q}_B^2 + 4\gamma^2\Omega_\pm^2 (\mathcal{C}_\pm - \frac{3}{4}\mathcal{D})] (\gamma\sigma)^2 + \hat{q}_B^2 [q_B^2 - 4 \{ \frac{3}{4}\gamma^2\mathcal{D}\Omega_\pm^2 \}] = 0 \quad (6)$$

where γ is the red-shift factor, $\mathcal{D} = g_{rr}^{-1}$, and $\mathcal{C}_\pm \equiv 1 - \frac{3}{r} \pm \frac{2a}{r^{3/2}}$ corresponds to the \mathcal{C} function of Novikov & Thorne (1973) for pro-grade (+) orbits. Regarding the electromagnetic stress, the only difference with the non-relativistic, incompressible analog is that the Alfvén speed is now weighted by the relativistic enthalpy of the fluid (Araya-Góchez 2002)

$$\rho v_{\text{Alf}}^2 \equiv \frac{1}{2} F^{\mu\nu} F_{\mu\nu}. \quad (7)$$

Factoring out the orbital frequency $u^\varphi/u^t \equiv \Omega_\pm = \pm(r^{3/2} \pm a)^{-1}$ and with $\gamma\sigma \equiv \Omega_\pm \hat{\sigma}$, one has

$$\hat{\sigma}^4 - [2\hat{q}_B^2 + \hat{\chi}_\pm^2] \hat{\sigma}^2 + \hat{q}_B^2 [\hat{q}_B^2 + 4\hat{\Lambda}] = 0 \quad (8)$$

where

$$\hat{\Lambda} \equiv -\left\{\frac{3}{4}\gamma^2\mathcal{D}\right\} \quad \text{and } \hat{\chi}_\pm^2 = 4\gamma^2 (\mathcal{C}_\pm - \frac{3}{4}\mathcal{D})$$

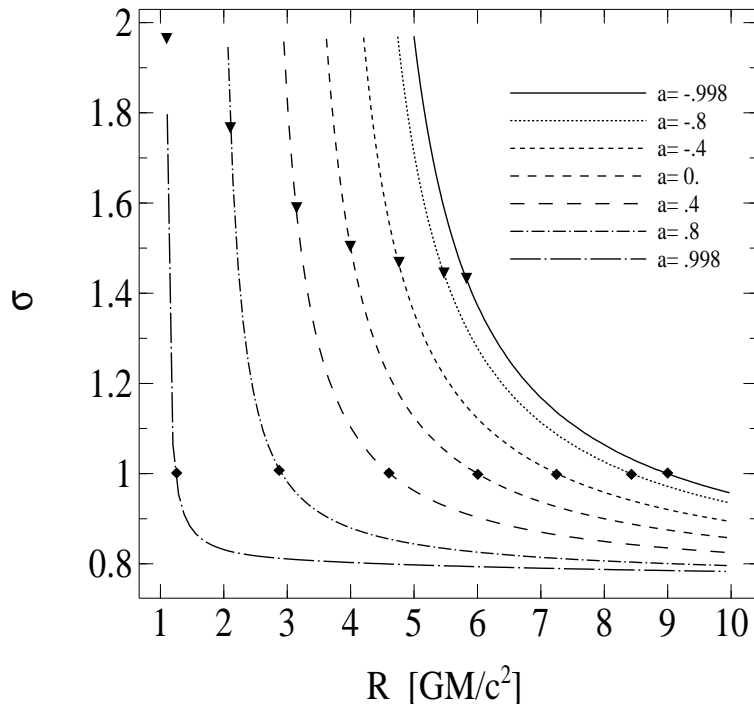


Figure 1. Normalized growth rate, $\hat{\sigma}$, as a function of radius for several values of the spin parameter a (from Araya-Góchez 2002).

denote the normalized shear parameter and co-moving epicycle frequency ($\frac{1}{\gamma} \hat{\chi}$ corresponds to the epicycle frequency as measured at asymptotic infinity). Thus, with the proper generalizations of the epicycle frequency and shear parameter, the local dispersion relation is identical with the Newtonian case in the limit of no fluid compression, c.f. Eqs [1&3] with $\Lambda \rightarrow 1$.

Next, using the relation $\gamma^2 = (1 \pm a/r^{3/2})^2 \mathcal{C}_{\pm}^{-1}$ for circular, geodesic flow (Novikov and Thorne 1973), one finds the fastest growing modes will conform with

$$\hat{q}_{\mathbf{B}}^2 = 1 - \frac{1}{16} \hat{\chi}^4 = 1 - \left(1 \pm \frac{a}{r^{3/2}}\right)^4 \left\{1 - \frac{3}{4} \frac{\mathcal{D}}{\mathcal{C}_{\pm}}\right\}^2 \quad (9)$$

which remains finite and close to the Newtonian value $\hat{q}_{\mathbf{B}} \rightarrow -\hat{\mathbf{A}}(2 + \hat{\mathbf{A}}) = 15/16$ for all radii outside of the ISCO.

Recall that the marginally stable orbit (a.k.a. the ISCO), r_{ms} , corresponds to the root of $\hat{\chi}_{\pm} = 0$. The radius of the circular photon orbit, r_{ph} , is where $\mathcal{C}_{\pm} = 0$ and the event horizon, r_+ , happens at the outer root of $\mathcal{D} = 0$. For any value of the rotation parameter a : $r_{\text{ms}} > r_{\text{mb}} > r_{\text{ph}} > r_+$. Our statement on large-scale effects follows from these remarks and from direct inspection of Eq [9]: $\hat{q}_{\mathbf{B}} \rightarrow 0^+$ as $r \rightarrow r_{\text{ph}}^+$, i.e. the most unstable MRI modes are go to large scales as the photon orbit is approached. Figs 1 & 2 show the general trends for the normalized growth rate and wave-numbers as functions of radius and spin parameter.

Two notable caveats of the relativistic approach involve the global disk structure and the compressibility of the modes. We discuss these in turn.

Curvature effects and radial field structure will indeed modify the dispersion relation² (see, e.g., Curry & Pudritz 1995, Ogilvie & Pringle 1996) but these effects are unlikely to modify the gross properties of the fastest growing modes unless radial stratification plays a destabilizing role. If such stratification were magnetically-driven; it would require an unlikely supra-thermal field $v_{\text{Aif}} \approx v^{\hat{\phi}} = \tilde{r}(\Omega - \omega)$, where $\tilde{r} \equiv r\mathcal{A}/\sqrt{\mathcal{D}}$ is the radius of gyration for the physical velocity in the locally non-rotating frame (Bardeen, Press & Teukolsky 1972). Furthermore, we note here and *correct* our previous comment (Araya-Góchez 2002): $\hat{q}_{\mathbf{B}} \rightarrow 0^+$ is merely a statement on the length-scale of the fastest growing modes, $k_{\parallel}^{-1} \simeq \mathcal{O}[\tilde{r}]$, regardless of field strength.

² the interested reader is invited to compare the relativistic, local version of the equations of motion for ξ : Eqs [32] of Araya-Góchez 2002, with the Newtonian, global version Eqs [2.6 & 2.7] of Ogilvie & Pringle 1996

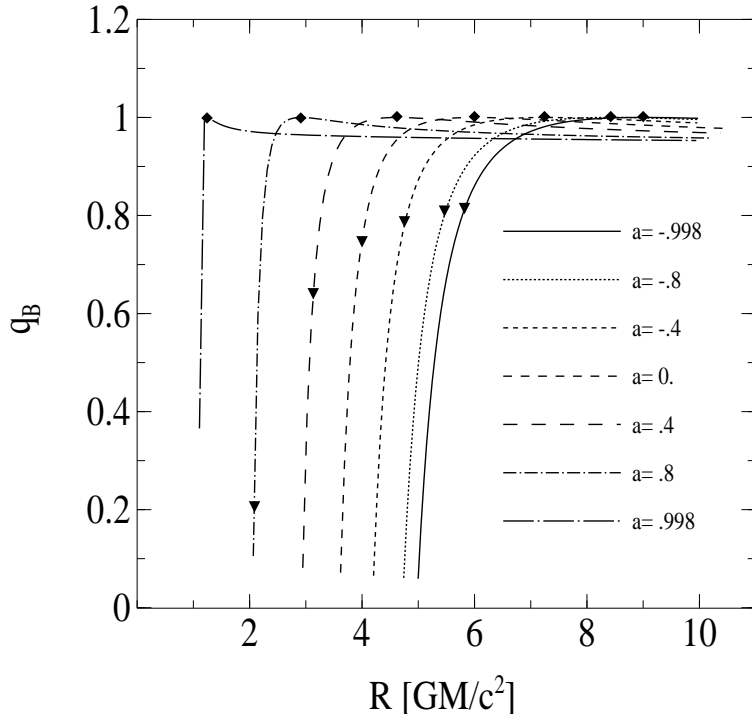


Figure 2. Normalized parallel wavenumber, \hat{q}_B , as a function of radius (in gravitational radii) for several values of the spin parameter a . Diamonds indicate the location of the marginally stable orbit, $\hat{\chi} \doteq \emptyset$, and triangles, the location of the marginally bound orbit (from Araya-Góchez 2002).

The compressibility of the modes alters the threshold of shear parameter where $\hat{q}_B \rightarrow 0^+$, but does not fundamentally affect the conclusions drawn from Eq [9] either. For roughly equal neutrino and radiation pressures (see below), one can use an effective adiabatic index (Araya-Góchez & Vishniac 2002) in Eq [4] to anticipate that the effects of compressibility on toroidal modes is to increment the threshold of shear parameter where $\hat{q}_B \rightarrow 0^+$ from $-\hat{A} = 2$ to $-\hat{A} \rightarrow 1 + 2D/(1 + \Lambda)$; c.f. Eq [4]. Nevertheless, since for geodesic flow $\hat{A} \propto D/C_{\pm}$ and $C_{\pm} \rightarrow 0$ @ r_{ph} , the increase in shear threshold in this setting is rather inconsequential.

3.3 Heat Conduction and Clump Scale

A precise assessment of radiative diffusion effects in the general relativistic regime is hampered by the breakdown of a key assumption made to simplify the “linear poking” on the Faraday field tensor (Araya-Góchez 2002): use of the enthalpy weighted specific four magnetic field in Eq [7]. However, just as in radiation pressure dominated fluids, one expects a neutrino stress dominated gas—with neutrinos semi-contained by the nucleon component through scattering—to comprise a rather peculiar MHD fluid. Indeed, when a fluid transitions into a radiative pressure regime, compressive modes will lose pressure support in a given range of wave-numbers (Agol & Krolik 1998). Thus, the magnetic field is truly frozen only to the co-moving volume associated with the baryon component and compressive perturbations need not behave adiabatically.

The half optical depth to scattering of a standard radiation-pressure-dominated α -disk is related to the scale height, \mathcal{H} , and rotation rate, Ω , by $\tau_{\text{disk}} = -c/(2\alpha\hat{A}\Omega\mathcal{H})$. This relation is explicitly sensitive only to the local nature of the cooling but is implicitly subject to a suitable vertical gradient of heat deposition (see, e.g., Krolik 1999). Therefore, these scalings also hold for a neutrino cooled α -disk through a replacement in the source of opacity by neutrino scattering in the non-advective accretion regime: $0.1 M_{\odot} \text{ sec}^{-1} \leq \dot{M} \leq 1 M_{\odot} \text{ sec}^{-1}$. On the other hand, in the Newtonian regime $\hat{q}_B \simeq \mathcal{O}[1]$ and for magnetic angular momentum transport such that $\alpha \simeq v_{\text{Aif}}^2/c_{\mathcal{H}}^2$, the depth through the MRI eddies is $\tau_{\text{eddy}} \sim v_{\text{Aif}}/c_{\mathcal{H}} \times \tau_{\text{disk}} \sim c/(2\hat{A}\sqrt{\alpha}c_{\mathcal{H}}) \gg 1$. Thus, assuming an isotropic random walk for neutrinos, the diffusion time through these eddies, $t_{\text{diff}} \sim \Omega^{-1}$, is similar to the time scale for fastest MRI modes to develop $t_{\text{MRI}} \simeq -A_{\text{Oort}}^{-1}$.

Radiative heat conduction will isotropize the dynamically dominant modes since neutrinos will diffuse through the smallest distance associated with the eddies, i.e. mostly in the vertical direction. In our problem, this will diminish the growth rate of

the instability (Blaes & Socrates 2001) but not by much. Indeed, if neutrino stress were predominant, the horizontal regime of fastest growth (e.g. §3.1) would be inaccessible; yet, such is never the case since the pressure contributions from radiation, pairs and neutrinos, all have the same temperature dependence $a/6 T^4$ with the relative contributions varying only by internal degrees of freedom times particle statistics factors (with only one helicity state for neutrino pairs): 2×1 , $4 \times 7/8$, and $6 \times 7/8$ respectively. Thus, p_ν is never greater than about $\simeq p_{\text{rad}}$ where $p_{\text{rad}} = 11/12 a T^4$ includes the pressure from pairs and photons.

Let's quantify these arguments in order to gauge the length scale of the clumps. At a very fundamental level, clump formation is intimately connected to the effects of radiative heat conduction out of compressive perturbations. This can be understood by writing down the polarization properties of the fastest growing modes in the horizontal regime: $\xi_r = -\sqrt{\Lambda} \xi_\varphi$ & $|\xi_\theta| \ll |\xi_r|$, and reading from Eq [3] that at the linear stage of the instability there exists a converging flow toward the Lagrangian displacement node of the modes (see Fig 2 of Foglizzo and Tagger 1995). In a fluid with entirely elastic (adiabatic) properties, the pressure perturbation associated with such compression will act as a restoring force to de-compress the fluid in the non-linear stage. On the other hand, when the fluid has radiative heat conduction properties on the scale of the density perturbations, no such restoring force persists on time scales longer than the inverse of the growth rate so the clumps will survive for longer times. Turner *et al.* (2001, 2003) report that in a standard radiation-pressure-dominated disk, when $p_{\text{rad}} \gtrsim p_{\text{gas}} \simeq p_{\text{B}}$, the non-linear outcome of the MRI is a porous medium with drastic density contrasts. Under nearly constant total pressure and temperature, the non-linear regime shows that density enhancements anti-correlate with azimuthal field domains—just as expected from the linear theory—and that turbulent eddies live for about a dynamical time scale while mass clumps are destroyed through collisions or by running through localized regions of shear on a similar time scale. Notably, the non-linear density contrasts may be quite large $\langle \rho_{\text{max}}/\rho_{\text{min}} \rangle \gtrsim \mathcal{O}[10]$. We make no attempt here to estimate $\Delta\rho/\rho$ from the linear theory but rather take the view that when the length scale of the instability is suitable large, $\lambda_{\text{MRI}} \simeq \mathcal{O}[\tilde{r}]$ (see below), a fraction of $\mathcal{O}[1/2\pi]$ of the mass in the annulus $r_{\text{mb}} \leq r \leq r_{\text{ms}}$ will reside in one massive clump such that the gravitational wave emission associated with the in-fall of this clump will dominate the power spectrum.

Let us emphasize that the isotropic size of the clumps is determined by the condition that, on the time scale of the instability, neutrinos will diffuse through the clumps *via* nucleon scattering and/or absorption followed by re-emission. For simplicity, we again assume local balance of dissipation from the shear flow with cooling from neutrino emission and a constant supersonic Mach number for the disk flow: $M_\varphi = v^{\tilde{\varphi}}/c_{\mathcal{H}}$ ($M_\varphi = 2.5$ is consistent with the results of PWF in the neutrino cooling regime). Under this assumption, we need not worry about detailed neutrino transport and, relaxing the condition $\hat{q}_{\text{B}} \approx 1$, the size of the most massive clumps will correspond to

$$l_{\text{clump}} \simeq v_{\text{AIf}}/c_{\mathcal{H}} \mathcal{H} \sim \sqrt{\alpha} M_\varphi^{-1} \tilde{r}.$$

Thus, in the relativistic regime the length-scale of the clumps will be smaller than the scale associated with the fastest growing modes by a factor of $\mathcal{O}[\hat{q}_{\text{B}}]$.

4 A SIMPLE PHYSICAL MODEL FOR GRAVITATIONAL WAVE EMISSION

The key to our argument for clumpy, near-hole hyper-accretion is based on the observation that the length-scale of the fastest growing modes may be quite large at the innermost disk boundary r_{mb} . Since the radial velocity is non-negligible, one cannot demand “tightly fitting” eigenmodes on the circumference at fixed radius. Loosely speaking, the WKB modes live on ingoing spiral trajectories (see §4.2); but we are only concerned with their overall gross properties.

The clumps form very rapidly, $t_{\text{MRI}}^{-1} \simeq \Omega \hat{\sigma}$, and very close to the horizon. Since these are very compact, $l/\tilde{r} \simeq \mathcal{O}[0.1]$, we considered them as point particles in the order of magnitude estimate of gravitational wave emission below. Computation of accurate waveforms for the in-fall of a single clump constitutes a daunting task because of the non-trivial multipole contributions to the radiation field in the strong gravity regime near r_{mb} . The contributions from higher than quadrupole will broaden the power spectrum of emitted waves (Zerilli 1970, Davis *et al.* 1971, hereafter DRPP) and recent results by Lousto & Price (1997, hereafter LP97) show that particles released from very near the marginally bound orbit of a non-spinning hole—or more precisely near the maximum of the Zerilli potential—will maximize the locally radiated energy.

As a “back of the envelope” estimate of the quadrupole r.m.s. strain, $|h| = \sqrt{h_+^2 + h_\times^2}$, associated with the in-fall of a single clump, we simply assume that the clump is formed above r_{mb} and that it survives for one rotation period before plunging into the hole. The transverse-traceless projection of the metric perturbation in the radiation zone, h_{ij}^{TT} , is estimated by replacing the second time derivative of the mass quadrupole moment, $\partial_t^2 \mathcal{J}_{ij}^{\text{TT}}$, by the kinetic energy associated with non-spherical motion; i.e., clump rotation as seen at asymptotic infinity (Thorne 1987). Thus

$$|h| = |h_{ij}^{\text{TT}}| \equiv \frac{2}{d} \left[\frac{G}{c^4} \right] |\partial_t^2 \mathcal{J}_{ij}^{\text{TT}}(t-r)| \simeq \left[\frac{G}{c^4} \right] \frac{\tilde{r}^2 \Omega^2}{d} \delta M \simeq \frac{G \delta M}{(c^2 d)}.$$

For a $15 M_\odot$ black hole rotating at $a = .98$, and accreting $1 M_\odot \text{ sec}^{-1}$, the mass in the clumps is $\delta M \simeq \dot{M}/\Omega \simeq 1.8_{-4} M_\odot$, where $\Omega(r_{\text{mb}}) \simeq .4 = 5400 \text{ Hz}$; corresponding to a linear frequency $\Omega(r_{\text{mb}})/\pi = 1720 \text{ Hz}$. This gives $|h| \simeq 3.2_{-25}$ for a source at 27 Mpc. To bring this into the LIGO band, $|h|_{\text{eff}} \simeq 1._{-21}$ one would need to integrate over $N \simeq 1._{+8}$ cycles or over 1700 sec.! Thus, the r.m.s. strain associated with in-fall of a single clump onto the hole is too small to be of any astrophysical importance at present.

But this issue is more subtle than it appears at first sight.

4.1 Quasi-normal Ringing Waveforms: Single Excitation Event

Since the clumps form in a strong gravity regime, the process of gravitational wave emission from in-fall at such a short range must be cast as an excitation of the infinite number of increasingly damped quasi-normal modes of oscillation of the background geometry (Leaver 1985). The often-drawn analogy for such quasi-normal ringing (QNR) of the hole to the ringing of a bell is fundamentally flawed in at least one respect: the black hole is not excited by the smashing of the clump as it “hits” the horizon. The hole is rather excited when the metric perturbation associated with the clump is “felt” by the background metric. The excitation event therefore constitutes a smooth process whereby in-fall of a clump from $\simeq r_{\text{mb}}$ and through r_+ serves as a source in the Teukolsky (1973) equation for small perturbations to the Kerr geometry (with appropriate boundary conditions at r_+ and r_∞). This is an important distinction with a great deal of relevance to the problem at hand since we need to gauge the “driving” of QNR modes in terms of an effective coupling from clump in-fall.

Clumpy black hole accretion from an exterior disk will excite preferentially quadrupole, bar-like mode perturbations of the geometry with spheroidal harmonic indices³ $(l, m) = (2, 2)$. An approximate analytical expression for the QNR frequency of this mode is given by Echeverria (1989):

$$\omega_{22} = [1 - 0.63(1 - a)^{3/10}] \times \left\{ 1 + \frac{i}{4}(1 - a)^{9/20} \right\}. \quad (10)$$

The corresponding quality factor, a.k.a. Q-value, of the (2,2) mode

$$Q_{22}(a) \equiv \frac{1}{2} \frac{\Re[\omega_{22}]}{\Im[\omega_{22}]} = 2(1 - a)^{-9/20}, \quad (11)$$

is $\geq 2\pi$ for $a_{\text{crit}} \geq 0.92$. This represents a minimum value of a to regard the hole as a decent bar-like-mode oscillator. Below a_{crit} the mode is damped too strongly to allow for any significant build up of the strain signal/spectrum from resonant accretion (see below).

In the radiation zone and time domain, undriven QNR waveforms constitute circularly polarized, damped oscillations (Leaver 1985, Echeverria 1989)

$$h(t) \equiv h_+ - ih_\times = \frac{H_0}{d} S_{22}(\phi, \theta, a) e^{-i(\omega_{22}t - \varphi)} \quad (12)$$

where d is the luminosity distance to the source, $S_{22}(\phi, \theta, a)$ is a spin weighted, normalized ($\int d\Omega |S_{22}|^2 = 1$), spheroidal harmonic of coordinates ϕ & θ [in the Schwarzschild limit $S_{22}(\phi, \theta, a \rightarrow 0) \rightarrow Y_{22}(\phi, \theta)$]. The strain length amplitude of the waveform, H_0 (in units of the hole’s mass M), and the phase shift, φ , depend on the initial conditions of the metric perturbation.

H_0 gauges the efficiency of the emission process to posit a fraction of the total rest-mass energy of the system into outgoing gravitational wave energy. For strong excitation events such as binary black hole coalescence, this fraction may be as large as 3% (see, e.g. Flanagan & Hughes 1998). For the in-fall of a clump of mass $\delta M \ll M$, this fraction scales as $\varepsilon(\delta M)^2/M$ (DRPP), with a corresponding time domain strain amplitude $\propto \sqrt{\varepsilon} \delta M / \sqrt{M}$. The precise value of ε for a rotating hole is unknown, but it hovers on a few per cent for the perturbations of a Schwarzschild geometry induced by radial in-fall from infinity⁴ (DRPP). For non-axisymmetric perturbations, the energy released from clump in-fall may be considerably larger (Fryer, Holtz & Hughes 2002) and for nearly resonant, driven oscillations from hyper-accretion, we demonstrate below that the total amount of energy deposited into outgoing gravitational waves is only bounded from above by a factor of a few times the rest-mass-energy of a single clump!

4.2 Collective Effects: Resonant Driving of QNR modes

To assess the free-fall stage of the clumps, we recall from §2 that the cusp in effective potential occurs somewhere above r_{mb} (depending on angular velocity profile) and that a relativistically hot accretion flow may possess a semi-Keplerian angular velocity profile, $\Omega_+ = (r^{3/2} + a)^{-1}$, down to this region, (PWF, Popham & Gammie 1998, Hawley & Krolik 2001). Parameterizing the accretion flow through its Mach number and the angular momentum transport through a Shakura & Sunyaev “ α ” parameter (as in §3.3, we adopt $M_\varphi \doteq 2.5$ & $\alpha \doteq 0.1$), when $a \gtrsim 0.9$ the wavelength associated with the fastest growing MRI modes becomes comparable with $2\pi\tilde{r}$ at a radius $r \geq r_{\text{mb}}$; e.g., when $\hat{q}_{\text{B}} \simeq .126\sqrt{\alpha_0.1} M_{\varphi, 2.5}^{-1}$. At higher spin parameter values, MRI modes go to comparably large scales at radii closer to r_{ms} . Thus, the annulus $r_{\text{ms}} \geq r \geq r_{\text{mb}}$ constitutes a relativistic locus for large-scale magneto-rotationally induced fluid dynamics at moderately large values of black hole spin: $a \geq 0.9$.

Since the radial velocity is non-negligible, MRI wave-modes must be interpreted as WKB modes that live on in-spiral trajectories. For the sake of simplicity in the discussion below, presume that fluid elements undergo one full rotation in the annulus $r_{\text{ms}} \geq r \geq r_{\text{mb}}$ before “plunging in” from r_{mb} . The integrated phase along this path can be interpreted with a skewed effective wavelength which goes to increasingly larger length-scales as fluid particles approach r_{mb} . If we demand a tight fit

³ Quadrupole perturbations, $l = 2$, are reckoned to contribute about 90% of the energy budget for outgoing GW’s while $l = 4$ modes add about 10%. Higher multipole contributions are negligible, see, e.g. DRPP, LP97.

⁴ Strictly speaking, the energy released in this case includes not just the ringing phase but also a small contribution from the gravitational Bremsstrahlung component, see, e.g., LP97.

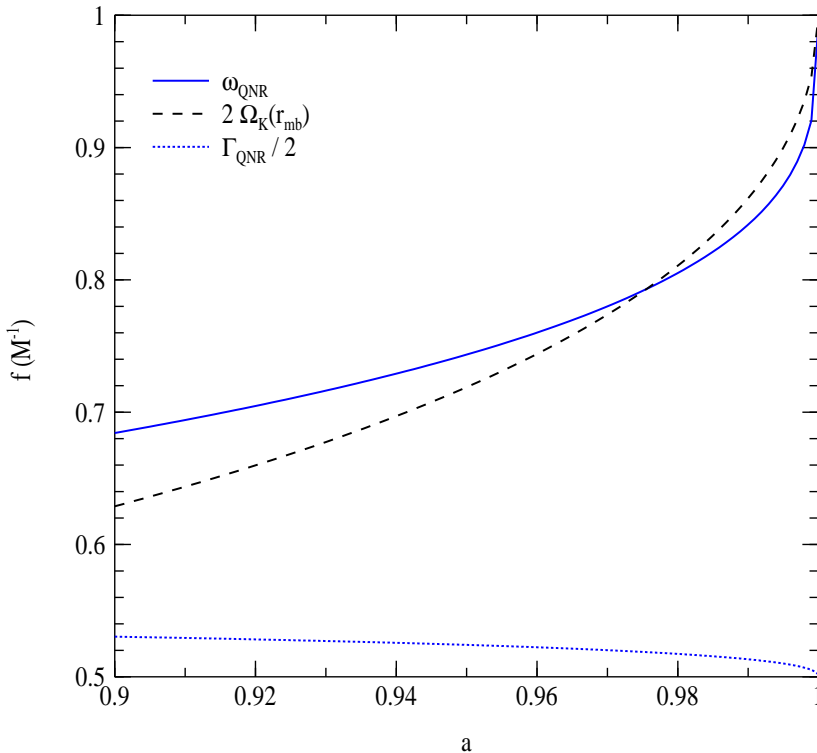


Figure 3. Shown are the real part of the QNR frequency, ω_{QNR} , and the driving frequency, $\omega_{\text{dr}} = 2\Omega_+(r_{\text{mb}})$, for quadrupole oscillations as functions of the hole’s spin parameter a . Plotted also is half of the imaginary part of the QNR frequency offset by +0.5 from zero for ease of comparison with the difference among the other two frequencies. Most notable is the fact that throughout the range $a \geq 0.95$, $|\omega_{\text{QNR}} - \omega_{\text{dr}}| \leq \frac{1}{2}\Gamma_{\text{QNR}}$ which implies resonant driving of the QNR modes from hyper-accretion.

of one whole, integrated WKB wavelength on the in-spiral trajectory between r_{ms} and r_{mb} , the mid Lagrangian displacement node, $\xi(\tau) = 0$, represents a converging point for the flow in the linear stage of the instability as seen by a co-moving geodesic observer. This node subsequently develops into the mass over-density that we identify with a clump in the non-adiabatic stage (i.e., when neutrinos have diffused out of the compressive perturbation, §3.3). Since the scale of the mode is larger downstream of the displacement node, most of the mass in the over-density will be advected in from fluid particles that rush upstream toward the node on the instability time scale; a smaller fraction of the clump’s mass flows downstream toward the node, from smaller scales upstream.

When the effective WKB scale on the instability is suitably large, a reasonably large fraction of the mass in the annulus will reside in a single clump by the time it reaches r_{mb} . The subsequential “free-fall” from r_{mb} (presuming this radius corresponds to the cusp in effective potential; e.g., Kozłowski *et al.* 1978, Abramowicz *et al.* 1978), occurs on a dynamical time scale: $t_{\text{dyn}} \equiv \Omega_+^{-1}(r_{\text{mb}})$. Furthermore, since l -pole modes couple to the l -multipole of the dynamical frequency (e.g., Ex. 3.7 of Rybicki & Lightman 1979), the driving frequency for quadrupole oscillations corresponds to twice the relativistic Keplerian frequency at r_{mb} : $\omega_{\text{dr}} \equiv 2\Omega_+(r_{\text{mb}})$. Remarkably, *the difference between the driving frequency and the resonant (2,2) QNR frequency resides within a factor of the order of the damping rate throughout the range $.9 \lesssim a \lesssim .99$* (Fig 3); whereas the Q value of the mode hovers on $5.6 < Q < 33$.

This picture of hyper-accretion would portray an ideal scenario to drive the QNR modes resonantly *were* the clumps to arrive at r_{mb} steadily, with a small spread around time intervals of $\mathcal{O}[\Omega_+^{-1}]$, and for long enough to build the strain amplitude up to a saturation point—or about $2Q$ cycles (see below). It is noteworthy that relativistic magneto-rotational dynamics (§2) indicates that mass over-densities form rapidly enough to feed the QNR modes of the hole efficiently. Yet, nature will add randomness to the process.

The added stochasticity in the arrival times of the clumps is related to the seed density perturbations in the flow. The accretion flow outside r_{ms} is turbulent on small scales, $\ell_{\text{turb}} \ll r$, and these density perturbations act as seeds for clump formation as these enter the relativistic annulus. This fact notwithstanding, in the picture of clump formation outlined above the probability distributions for arrival times and clump mass are strongly affected by large scale magneto-rotational dynamics

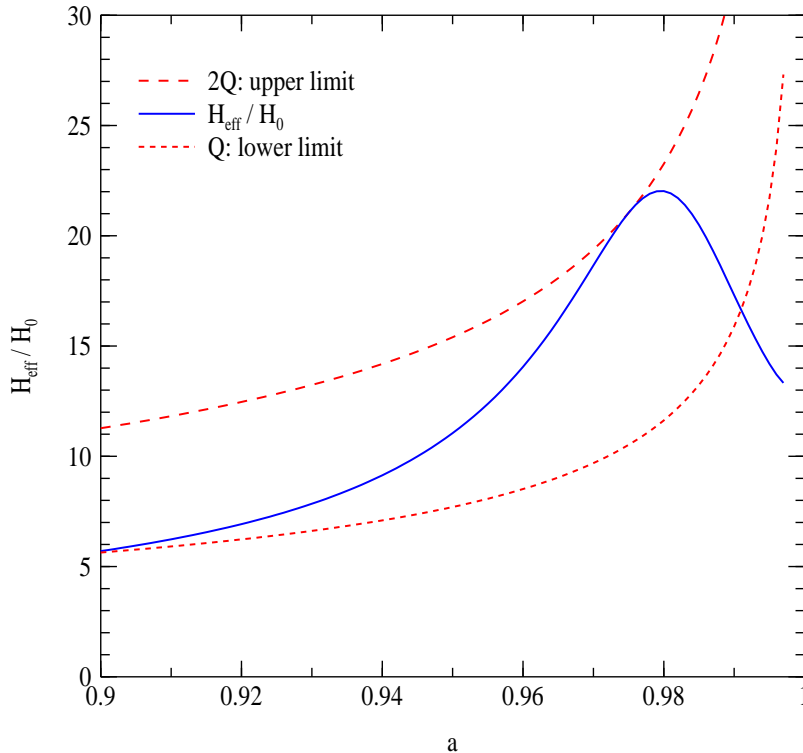


Figure 4. The solid line indicates the augmented amplitude of QNR oscillations driven near resonance by clumpy hyper-accretion from a neutrino-cooled disk as a function of the hole’s spin parameter a . Modulo a small spread caused by the stochasticity in time arrival of the clumps to r_{mb} (see discussion in the text), the enhanced amplitude lies within the curves for $Q(a)$ and $2Q(a)$ throughout the range $a > .9$. A brisk energy deposition rate $\propto (H_{\text{sat}}/H_0)^2$ ensues.

near r_{mb} . If the flow is steady, large scale dynamics should minimize the impact of small scale perturbations upstream *and* induce a correlation between the two distributions. Below, we simply assume that the probability distribution for arrival times will favor resonant driving of the modes with a moderate spread around the resonant frequency of arrival times (see further discussion on this point below). Lastly, note that the arguments above do not depend on in-spiral trajectories wrapping around fully on the annulus; since the MRI time scale is suitable fast, a small delay to reach the free-fall stage is all that is needed for MRI dynamics to act.

Beyond an initial transient period where the amplitude of the oscillation builds up to a saturation point, driven QNR oscillations become *undamped* oscillations at the driving frequency

$$h(t) = \frac{H_0}{d} \frac{\omega_{\text{QNR}}^2}{\omega_{\text{dr}}^2 - \omega_{\text{QNR}}^2 - i\omega_{\text{dr}}\Gamma_{\text{QNR}}} S_2^2(\phi, \theta, a) e^{-i\omega_{\text{dr}}t} \equiv \frac{H_{\text{sat}}}{d} S_{22}(\phi, \theta, a) e^{-i(\omega_{\text{dr}}t + \delta_t)}, \quad (13)$$

where $\delta_t = \tan^{-1}(\omega_{\text{dr}}\Gamma_{\text{QNR}}/[\omega_{\text{dr}}^2 - \omega_{\text{QNR}}^2])$ is a slowly varying function of time and the saturation amplitude, H_{sat} , represents an effective strain length (in units of the system’s total mass M) set by the condition that the energy input from clump in-fall ($\propto H_{\text{sat}}$) be balanced by the damping losses ($\propto H_{\text{sat}}^2$). When the driving frequency is near resonance, H_{sat} is limited primarily by the natural⁵ damping of the QNR mode, $\Gamma_{\text{QNR}} \equiv \Im[\omega_{22}]$, and secondarily by the relative difference of the driving frequency to the resonant frequency for quadrupole ringing, $\omega_{\text{QNR}} \equiv \Re[\omega_{22}]$. Furthermore, since $\omega_{\text{dr}} \approx \omega_{\text{QNR}}$ for a relatively broad range of a values (Fig 3), the resonant frequency may be taken to be ω_{QNR} .

The energy flux carried by driven QNR waveforms benefits greatly from the build up in the amplitude of the strain, H_{sat} , when compared to the ringing from a single excitation event H_0 (c.f., Eq [12]). Indeed, when driven near resonance the augmented amplitude is proportional to twice the Q value of the mode: $H_{\text{sat}}|_{\omega_{\text{dr}}=\omega_{\text{QNR}}} = 2Q H_0$ (c.f. Eq [11]). Although the

⁵ Quasi-normal modes are strongly damped because of the B.C. of purely ingoing radiation at r_+ which saps most of the energy emitted by the metric perturbation unless the waves are strongly beamed from relativistic motion (Sterl Phiney, Priv. Comm.). In this sense, the damping of the mode corresponds to radiation reaction with most of the energy being advected in by the hole.

modes are driven precisely at resonance only for $a \approx .98$, note from Fig 3 that $|\omega_{\text{QNR}} - \omega_{\text{dr}}| \leq \Gamma_{\text{QNR}}$ throughout the range $.90 \lesssim a \lesssim .99$. This sets a lower bound on the augmented strain amplitude for this range of a : $H_{\text{sat}}/H_0 \gtrsim Q$ (recall that the resonant denominator only looks like a Lorentzian very near the resonance). Fig 4 shows the exact value of the augmented strain amplitude for $a \geq .9$. Furthermore, adopting a very modest $\varepsilon_0 = .02$ for the in-fall of a single clump (in accordance with the DRPP and LP97 results; see also discussion in §4.1), the augmented efficiency factor in GW energy deposition from driven oscillations $\varepsilon = (H_{\text{sat}}/H_0)^2 \varepsilon_0$ may be larger than unity. Depending on the hole’s spin, $\varepsilon \simeq 1 - 10$ for $.92 \leq a \leq .98$ (c.f. Fig 4).

Next, let us relate the energy emitted by the sequential in-fall of N clumps of mass δM through r_+ to the amplitude of the waveform in the time domain. Assume N to be small enough such that $N\delta M < M_{\text{initial}}$ but large enough to enable a sensible average of the RMS strain amplitude over the corresponding number of wave cycles. The energy flux averaged over N cycles is (Isaacson 1968)

$$\frac{dE}{dAdt} = \left[\frac{c^3}{G} \right] \frac{1}{16\pi} \langle \dot{h}(t) \cdot \dot{h}^*(t) \rangle. \quad (14)$$

With $h(t)$ as given by Eq [13] and assuming no spin evolution, $\dot{a} \doteq \emptyset$, the total energy radiated in gravitational waves results from integrating Eq [14] over an encompassing surface (recall $\int d\Omega |S_{22}|^2 = 1$), and over a time interval corresponding to N cycles of ω_{dr} :

$$E_{\text{GW}} = \left[\frac{c^3}{8G} \right] N \omega_{\text{dr}} |H_{\text{sat}}|^2. \quad (15)$$

On the other hand, an approximate estimate of the total GW energy deposition which accounts for a slight mass increment of the black hole without spin evolution is as follows. First, write the energy emitted during one driven cycle as follows $\delta E = [c^2] (\varepsilon \delta M) \delta M / M_{\text{initial}}$, and note that the clump mass $\delta M \simeq \dot{M} \Omega_+^{-1}(r_{\text{mb}}) \propto M$ (constant a and \dot{M}). For $\Delta M \equiv \Sigma \delta M < M_{\text{initial}}$, replace the factor in parenthesis by the geometric mean of δM over the hyper-accreting epoch, $\delta \bar{M}$, and perform the integral of $\delta M / M(t)$ by writing $\delta M = \dot{M} dt$. This yields

$$\Delta E_{\text{GW}} = [c^2] \varepsilon \delta \bar{M} \ln \left(\frac{M_{\text{final}}}{M_{\text{initial}}} \right) \quad (16)$$

where ε may be larger than unity for black hole spins in excess of $a \gtrsim .92$.

5 DETECTABILITY CRITERION

Rather than attempt to describe the complex time evolution of the gravitational waveform throughout the hyper-accreting stage, we will simply assess the detectability of the waves with the matched filtering technique by utilizing the above energy estimate, Eq [16], while focusing on a relatively short time interval such that the added mass to the hole is a small fraction of the initial mass.

For definiteness, we adopt $M_{\text{initial}} = 15 M_{\odot}$ ($f \simeq 2147$ Hz) and $\Delta M = 1 M_{\odot}$ corresponding to a second of hyper-accretion at $\dot{M} = 1 M_{\odot} \text{ sec}^{-1}$. Under the simplified model for clump mass probability distribution as outlined above (quasi-linear analysis), a large fraction of the mass in the locus $r_{\text{mb}} \leq r \leq r_{\text{ms}}$ at any given time resides in a clump by the time fluid particles reach r_{mb} . We estimate the mass in this clump to be $\delta M = \dot{M} \Omega_+^{-1}(r_{\text{mb}})$ which is a factor of 2π smaller than the total mass in the annulus for fully wrapping, in-spiral trajectories, §4.2.

We follow Flanagan & Hughes (1998) to evaluate the likelihood of detection of GW from driven QNR modes by the LIGO interferometers. The criterion for detectability of the wave train through the matched filtering technique is a non-trivial S/N ratio

$$\langle [S/N]^2 \rangle = \int d \ln \omega \frac{h_{\text{char}}^2(\omega)}{h_{\text{noise}}^2(\omega)} \quad (17)$$

where $h_{\text{noise}}(\omega)$ ($= h_{\text{noise}}(f)/\sqrt{2\pi}$) reflects the detector spectral density of strain noise appropriately averaged for random incident orientations with respect to the LIGO interferometers. The characteristic strain amplitude of the wave train is given by

$$h_{\text{char}}^2(\omega) \equiv \frac{2(1+z)^2}{\pi^2 d^2} \frac{dE}{d\omega} [(1+z)\omega], \quad (18)$$

where d is the luminosity distance to the source, z the redshift, and ω the observed angular frequency. Defined this way, h_{char} is not trivially related to the amplitude of the strain in the time domain, H_{sat} , nor to the same in the frequency domain. It is rather a gauge of the time integrated power spectrum weighted by the “mono-chromaticity” of the wave train over the observation time.

With $(1+z)\omega \rightarrow \omega$, the GW energy spectrum from driven QNR modes in the radiation zone,

$$\frac{dE(\omega)}{d\omega} = \frac{\omega^2}{16\pi^2} \tilde{H}(\omega) \cdot \tilde{H}^*(\omega), \quad (19)$$

ensues from a Fourier transform of the strain signal in the time domain as given in Eq [13] (compare this expression with Eq [2.38] of Flanagan & Hughes 1998, and note the conforming notation used throughout).

Let us approximate all quantities $\propto M$ by their geometric mean and assume no spin evolution during a small epoch of hyper-accretion $T = 2\pi N/\omega_{\text{dr}}$ (with $\log N$ in the range 3-3.5). With $\tilde{H}(\omega) = 2H_{\text{sat}}e^{i\delta t} \sin[N\pi\Delta\omega/\omega_{\text{dr}}]/\Delta\omega$ (note that $\dot{a} \doteq 0 \Rightarrow \delta t = \text{constant}$ as well), the characteristic strain amplitude of driven QNR waves turns out to be

$$h_{\text{char}}^2(\omega) \equiv \frac{8(1+z)^2 H_{\text{sat}} \cdot H_{\text{sat}}^*}{(2\pi)^4 d^2} \left[\frac{N\pi\omega}{\omega_{\text{dr}}} \frac{\sin(x-b)}{x-b} \right]^2 \quad (20)$$

where $x-b \equiv N\pi(\omega - \omega_{\text{dr}})/\omega_{\text{dr}}$.

The strength of the characteristic strain signal at the driving frequency $\omega = 2\Omega_+(r_{\text{mb}})$ follows by setting the expression in the square parenthesis to $[N\pi]^2$ and by utilizing Eq [15] to replace $|H_{\text{sat}}|^2$ in favor of the energy released during the hyper-accreting epoch ΔE_{GW} as given by Eq [16]

$$h_{\text{char}}^2|_{\omega=\omega_{\text{dr}}} = \left[\frac{G}{c^3} \right] \left(\frac{2(1+z)}{\pi d} \right)^2 \frac{N\Delta E_{\text{GW}}}{\omega_{\text{dr}}} = \left[\frac{G}{2\pi c} \right] \left(\frac{2(1+z)}{\pi d} \right)^2 \varepsilon \delta \bar{M} T \ln \left(\frac{M_{\text{final}}}{M_{\text{initial}}} \right). \quad (21)$$

For GRB 030329, we plug in $z = .1685$, $d = 810\text{Mpc}$ ($H_0 = 70$, $\Omega_b = .3$, $\Omega_v = .7$), $M_{\text{initial}} = 15 M_{\odot}$, $T = 1$ sec, and $\delta \bar{M} = \dot{M}\Omega_+^{-1}(r_{\text{mb}}) \simeq 1.83_{-4} M_{\odot}$ and choose $a = .98$ ($H_{\text{sat}}/H_0 = 22$) to obtain $h_{\text{char}} \simeq 8.4_{-23}$ at the observed linear frequency $f = 1490\text{Hz}$. Utilizing similar parameters for GRB980425 at $d = 27\text{Mpc}$, turns out a characteristic signal $h_{\text{char}} \simeq 2.16_{-21}$ at $f \simeq 1741\text{Hz}$.

6 DISCUSSION

We have laid out a physical—if simple minded—model for resonant driving of the quasi-normal ringing (QNR) wave modes of the Kerr geometry. A nascent black hole hyper-accreting at rates $\dot{M} \approx 1 M_{\odot} \text{sec}^{-1}$ from a neutrino cooled disk is reckoned to oscillate near resonance of its $(l, m = 2, 2)$ quadrupole QNR frequency due to the in-fall of compact mass over-densities from the cusp in effective potential on a dynamical time scale. This model is based on large-scale, magneto-rotationally-induced fluid dynamics in the ultra-relativistic region of the flow bounded from below by the marginally bound orbit radius: r_{mb} (assumed to coincide with the aforementioned cusp). The exact location of the cusp will change the dynamical time scale for in-fall but not by much when the spin parameter $a \geq .9$. Furthermore, since the MRI time scale is suitable fast, a small delay to reach the free-fall stage is all that is needed for MRI dynamics to act. Heat conduction from neutrino diffusion out of mass over-densities on the time scale of the instability warrants that compressive perturbations behave non-adiabatically. This leads to sufficiently long-lived clumps in a highly intermittent medium. When the spin parameter of the hole exceeds 90%, large-scale magneto-rotational wave modes will segregate compact matter over-densities from large-scale magnetic field domains. The subsequent in-fall of these clumps from r_{mb} will drive the QNR modes of the geometry in resonant fashion if the clumps arrive to r_{mb} steadily, with a small spread around time intervals of $\mathcal{O}[\Omega_+^{-1}]$, and for long enough to build the strain amplitude up to a saturation point.

It is difficult to address the probability distribution for clump arrival times from the linear theory alone but one anticipates that it will involve a co-moving time scale of $\mathcal{O}[\Omega_+^{-1}]$ and the integrated, spin dependent WKB wavelength on the inspire trajectory toward r_{mb} . We have argued that for large mass clumps, $\delta \bar{M} \simeq \dot{M}\Omega_+^{-1}$, the arrival times to r_{mb} will not be entirely stochastic since “the bucket needs time to fill-up”, nor entirely coherent since the seed density perturbations are stochastic but large-scale MRI dynamics will work to minimize the impact of this initial small-scale randomness. If the arrival times were entirely stochastic, the enhancement in energy deposition would be roughly proportional to the Q value of the mode instead of to Q^2 and the corresponding signal would be smaller by about an order of magnitude. A detailed probability distribution of arrival times requires an accurate account of the radial velocity profile and of the effective, spin-dependent WKB wavelengths on in-spiral trajectories which is beyond the scope of this study.

If the QNR modes are fed resonantly for a few seconds of hyper-accretion, the enhanced amplitude of the oscillations yields a very high rate of energy deposition into gravitational waves. Indeed, the integrated energy deposition is large enough to “evaporate” the equivalent of a factor of a few times the total rest-mass-energy of a single clump into gravitational waves. Yet, the characteristic frequency of emission resides on a less than optimal range with respect to the advanced LIGO noise curve: $f \simeq 8000 - 1600\text{Hz}$ for $M \simeq 3 - 15 M_{\odot}$. On the other hand, the high quality and coherence of the expected signal should make this model a prime candidate for narrow-band LIGO searches. For gamma-ray bursts at low redshifts, this may ultimately lead to a signal strong enough to be seen by LIGO II.

A $15 M_{\odot}$ black hole accreting at $1 M_{\odot} \text{sec}^{-1}$ may come about from the death throes of a very massive star. If such an explosion is associated with a long GRB, and the broad properties of the prompt gamma-ray light curve, to inner engine activity; hyper-accretion onto this heavy weight, fast spinning hole should be associated with a second broad hump in the light curve. We anticipate that gravitational waves with the predicted properties may be present at this stage of the GRB. The proposed mechanism is thus a direct probe of the elusive inner engine of gamma-ray bursts.

ACKNOWLEDGMENTS

It is a great pleasure to acknowledge stimulating and instructive discussions with Sterl Phinney, Lee Lindblom, Kip Thorne, Ethan Vishniac and Roger Blandford. I am greatly indebted with the TAPIR Group at Caltech for their hospitality and to Don Juan's teachings; "...because the warrior, having chosen a path, has but one goal: to traverse its full length."

REFERENCES

- Abramowicz, M., Jaroszynski, M. & Sikora, M. 1978, *A&A*, 63, 221
 Agol, E. & Krolik, J. 1998, *Ap.J.*, 507, 304.
 Araya-Góchez, R.A. 2002, *M.N.R.A.S.* 337, 795
 Araya-Góchez, R.A. & Vishniac, E.T. 2002, *M.N.R.A.S.* submitted (astro-ph/0208007)
 Balbus, S.A. & Hawley, J.F. 1991, *Ap.J.* 376, 214
 Balbus, S.A. & Hawley, J.F. 1992, *Ap.J.* 392, 662
 Balbus, S.A. & Hawley, J.F. 1998, *Rev. Mod. Phys.* 70, 1
 Bardeen, J., Press, W. & Teukolsky, S. 1972, *Ap.J.*, 178, 347
 Blaes, O. & Socrates, A. 2001, *Ap.J.*, 553, 987
 Blandford R. & Begelman M. 1999, *M.N.R.A.S.*, 303, L1
 Blandford R. & Begelman M. 2003 *M.N.R.A.S.* submitted (astro-ph/0306184)
 Curry, C. & Pudritz, R. 1995, *Ap.J.*, 453, 697
 Davis, M., Ruffini, R., Press, W. & Price, R. 1971, *Phys. Rev. Lett.*, 27, 1466
 Di Matteo, T., Perna, R. & Narayan, R. 2002, *Ap.J.*, 579, 706
 Echeverria, F. 1989, *Phys. Rev. D*, 40, 3194
 Flanagan, E. & Huges, S. 1998, *Phys. Rev. D*, 57, 4535
 Foglizzo, T. 1995, Ph.D. Thesis, University of Paris VII
 Foglizzo, T. & Tagger M. 1995, *A.&A.*, 301, 293
 Fryer, C., Holz, D. & Hughes, S. 2002, *Ap.J.*, 565, 430 (astro-ph/0106113)
 Gammie, C.F. & Popham, R. 1998, *Ap.J.*, 498, 313
 K.S Thorne 1987, in *300 Years of Gravitation*
 eds: S. Hawking & R. Israel Cambridge Univ. Press
 Hawley, J.F. & Balbus, J.H 2002, *Ap.J.*, 573, 738
 Hawley, J.F. & Krolik, J.H 2001, *Ap.J.*, 548, 348
 Hawley, J.F. & Krolik, J.H 2002, *Ap.J.*, 566, 164 & *Ap.J.* 573, 754
 Isaacson, R.A. 1968, *Phys. Rev.*, 166, 1272
 Kozłowski, M., Jaroszynski, M. & Abramowicz, M. 1978 *A&A*, 63, 209
 Krolik, J.H. 1999, *Active Galactic Nuclei: from the Central Black Hole to the Galactic Environment*
 Princeton Series in Astrophysics, Eds. Jeremiah P. Ostriker & David N. Spergel (Princeton: Princeton University Press)
 Leaver, E.W. 1985, *Proc. R. Soc. Lond. A* 402, 285
 Lousto & Price 1997, *Phys. Rev. D* 55, 2124L
 Narayan, R. & Yi, I. 1995a, *Ap.J.*, 444, 231; 1995b, *Ap.J.*, 452, 710
 Narayan, R., Igumenshchev, I. & Abramowicz, M. 2000, *Ap.J.*, 539, 798;
 Novikov, I. & Thorne, K. 1973, in *Black Holes*
 eds. C. DeWitt & B.S. DeWitt (New York: Gordon & Breach), 343
 Ogilvie, G.I. & Pringle, J.E. 1996, *M.N.R.A.S.*, 279, 152
 Popham, R. & Gammie, C.F. 1998, *Ap.J.*, 504, 419
 Popham, R., Woosley, S., & Fryer, C. 1999, *Ap.J.*, 518, 356
 Rybicky, G. & Lightman, A. 1979 *Radiative Processes In Astrophysics*
 John Wiley & Sons, Inc
 Shakura, N.I. & Sunyaev, R.A. 1973, *A&A*, 24, 337
 Teukolsky, S. 1973, *Ap.J.*, 185, 635
 Turner, N., Stone, J., & Sano, T. 2001 (astro-ph/0110272)
 Zerilli 1970, *Phys. Rev. D*, 2, 2141